ORIGINAL ARTICLE

Cancer Science WILEY

Targeting chemoresistance in Xp11.2 translocation renal cell carcinoma using a novel polyamide–chlorambucil conjugate

Shintaro Funasaki[1] | **Sally Mehanna**[1] | **Wenjuan Ma**[1] | **Hidekazu Nishizawa**[1,2] | **Yasuhiko Kamikubo**[3] 🟢 | **Hiroshi Sugiyama**[4] | **Shuji Ikeda**[4] | **Takanobu Motoshima**[2] | **Hisashi Hasumi**[5] 🟢 | **W. Marston Linehan**[6] | **Laura S. Schmidt**[6,7] | **Chris Ricketts**[6] | **Toshio Suda**[8,9] | **Yuichi Oike**[10] | **Tomomi Kamba**[2] | **Masaya Baba**[1] 🟢

[1]Laboratory of Cancer Metabolism, International Research Center for Medical Sciences (IRCMS), Kumamoto University, Kumamoto, Japan

[2]Department of Urology, Graduate School of Medical Sciences, Kumamoto University, Kumamoto, Japan

[3]Department of Human Health Science, Graduate School of Medicine, Kyoto University, Kyoto, Japan

[4]Department of Chemistry, Graduate School of Science, Kyoto University, Kyoto, Japan

[5]Department of Urology, Graduate School of Medicine, Yokohama City University, Yokohama, Japan

[6]Urologic Oncology Branch, National Cancer Institute, National Institutes of Health, Bethesda, Maryland, USA

[7]Basic Science Program, Frederick National Laboratory for Cancer Research, National Cancer Institute, Frederick, Maryland, USA

[8]Laboratory of Stem Cell Regulation, International Research Center for Medical Sciences (IRCMS), Kumamoto University, Kumamoto, Japan

[9]Cancer Science Institute of Singapore, Centre for Translational Medicine, National University of Singapore, Singapore City, Singapore

[10]Department of Molecular Genetics, Graduate School of Medical Sciences, Kumamoto University, Kumamoto, Japan

Correspondence
Masaya Baba, International Research Center for Medical Sciences, Kumamoto University, 2-2-1 Honjo, Chuo-ku, Kumamoto 860-0811, Japan.
Email: babam@kumamoto-u.ac.jp

Abstract

Renal cell carcinoma with Xp11.2 translocation involving the *TFE3* gene (TFE3-RCC) is a recently identified subset of RCC with unique morphology and clinical presentation. The chimeric PRCC-TFE3 protein produced by Xp11.2 translocation has been shown to transcriptionally activate its downstream target genes that play important roles in carcinogenesis and tumor development of TFE3-RCC. However, the underlying molecular mechanisms remain poorly understood. Here we show that in TFE3-RCC cells, PRCC-TFE3 controls heme oxygenase 1 (HMOX1) expression to confer chemoresistance. Inhibition of HMOX1 sensitized the PRCC-TFE3 expressing cells to genotoxic reagents. We screened for a novel chlorambucil–polyamide conjugate (Chb) to target PRCC-TFE3-dependent transcription, and identified Chb16 as a PRCC-TFE3-dependent transcriptional inhibitor of HMOX1 expression. Treatment of the patient-derived cancer cells with Chb16 exhibited senescence and growth arrest, and increased sensitivity of the TFE3-RCC cells to the genotoxic reagent etoposide. Thus, our data showed that the TFE3-RCC cells acquired chemoresistance through HMOX1

Abbreviations: AKT, AKT serine/threonine kinase; Ca^{2+}, calcium ions; Chb, chlorambucil–polyamide conjugate; Dox, doxycycline; ETP, etoposide; GPNMB, glycoprotein nonmetastatic B; H_2O_2, hydrogen peroxidase; HK2, hexokinase 2; HMOX1, heme oxygenase 1; P70 S6K, Ribosomal protein S6 kinase beta-1; PI, pyrrole imidazole; *Ret*, *Ret* proto-oncogene; SASP, senescence-associated secretory phenotype; TFE3, transcription factor binding to IGHM enhancer 3; TFE3-RCC, Xp11.2 translocation renal cell cancer.

expression and that inhibition of HMOX1 by Chb16 may be an effective therapeutic strategy for TFE3-RCC.

KEYWORDS
chemoresistance, HMOX1, PRCC-TFE3, pyrrole imidazole polyamides, Xp11.2 translocation renal cell carcinoma (TFE3-RCC)

1 | INTRODUCTION

Renal cell carcinoma associated with the Xp11.2 translocation (TFE3-RCC) is a recently identified subset of renal carcinoma with distinctive morphological characteristics common to papillary RCCs.[1–3] TFE3-RCC are more common in pediatric patients, comprising from 25% to 40% of cases in children and young adults compared with 2%–5% of adult cases.[4,5] The *TFE3* gene located at Xp11.2 forms a fusion protein, which is thought to play an important role in carcinogenesis and tumor development in TFE3-RCC.[2] Several *TFE3* chimeras, including *PRCC-TFE3*, *ASPSCR1-TFE3*, *SFPQ-TFE3*, *NONO-TFE3*, *RBM10-TFE3*, and *CLTC-TFE3* have been found to be clinically associated with TFE3-RCC.[2,6–9] All of the chimeric *TFE3* genes identified in TFE3-RCC are known to retain the TFE3 DNA binding and transcriptional motif, and clinical data have shown that all the TFE3 fusion proteins accumulate in the nucleus, indicating that these fusion proteins are highly activated within the tumor and act as oncogenes.[6,9,10] Thus, transcriptional regulation of the TFE3 fusion proteins is an important molecular mechanism that contributes not only to tumor development but also to the malignant characteristics of TFE3-RCC.

TFE3 is a member of the MiT family of transcription factors that controls multiple genes involved in lysosome biogenesis, autophagy, and cellular energy homeostasis, and have key roles in these cellular functions.[11–14] In addition, TFEB, another MiT family member, has also been shown to be involved in cell-cycle progression by modulating p21 or CDK4/Rb.[15,16] Both TFE3 and TFEB are stabilized in response to DNA damage stress through activation of the p53 transcriptional program.[17] TFE3 and TFEB transcription, together with the p53 axis, coordinate to induce apoptotic cell death more efficiently.[17] The broad functionality of the MiTF/TFE3/TFEB transcription factor family suggests that the hyperactive nature of the TFE3 fusion proteins is responsible for the growth phenotypes in these tumors. To what extent TFE3-RCC tumor survival is dependent on the transcriptional activity of the TFE3 fusion proteins remains unknown.

We have recently generated a model of Xp11.2 translocation RCC by targeted the expression of *PRCC-TFE3* in mouse kidneys and showed that the mouse model develops kidney tumors with similar morphological characteristics to human TFE3-RCC.[18] Analyzing the mouse model and PRCC-TFE3 expressing cells derived from the patient, we confirmed that GPNMB is a direct target of PRCC-TFE3 and showed that inhibition of the *Ret* pathway, which is upregulated in the mouse PRCC-TFE3 kidney tumor, ameliorated tumor

cell growth *in vivo*.[18] In this study, we further analyzed the transcriptome data from Xp11.2 tRCC mouse kidneys by focusing on the pathways controlled by PRCC-TFE3 transcription. Our analyses revealed that PRCC-TFE3 expressing mouse kidneys demonstrated a p53 pathway enrichment, as well as an apoptosis signature. We identified HMOX1 (heme oxygenase 1) as a downstream transcriptional target of PRCC-TFE3, and showed that HMOX1 expression confers chemoresistance against various genotoxic stresses such as reactive oxygen species (ROS) and etoposide in PRCC-TFE3 expressing cells. Here we designed a novel chemical inhibitor based on chlorambucil-conjugated PI polyamide (Chb) to inhibit PRCC-TFE3 transcription, and showed that combination treatment of Chb16 with a cancer drug has a synergistic effect that enhances cytotoxicity in TFE3-RCC, thereby suggesting a potential use in TFE3-RCC therapy.

2 | MATERIALS AND METHODS

2.1 | Cell culture

HK2 cell lines that express HA-PRCC-TFE3 in a doxycycline-dependent manner have been described previously.[19] HEK293 cell lines expressing HA-PRCC-TFE3 in a doxycycline-dependent manner were established using the Flp-In T-Rex System (Invitrogen).[18] The patient-derived TFE3-RCC cell lines, UOK120, UOK124, and UOK146 cell harboring PRCC-TFE3 translocation have been described previously[18] and were cultured in DMEM 10% FCS. *PRCC-TFE3*, *p53*, or *p21* knockdown was done using MiRE-based shRNA plasmid vectors. Briefly, SGEP plasmid (Addgene #111170) vectors were cloned with shRNA-miRE sequences as described previously.[20] TFE3-RCC cell lines were infected with the viral supernatants, and the infected TFE3-RCC cells were selected with puromycin (Promega). The target sequences used for constructing shRNA-miRE are as follows:

> shTFE3#1 5-TCAGATAAACAAATGAGGGGGT-3;
> shTFE3#3 5-TATTATTTTAATCACAAACCTA-3;
> shp53#1 5-TCCACTACAACTACATGTGTAA-3;
> shp21#1 5-CTCAGTTTGTGTGTCTTAATTA-3.

For HMOX1 knockdown, the MISSION shRNA (TRCN0000290435 or TRCN000029043; Sigma) lentivirus plasmid vector (pLKO.1) was used.

2.2 | Chemical synthesis

PI polyamides were prepared in a stepwise reaction using the Fmoc solid-phase protocol as previously reported.[21] Oxime resin was used for all syntheses. Chb 16 was prepared in accordance with a synthetic procedure previously reported.[1] The PI polyamide with oxime resin was cleaved using *N,N*-dimethyl-1,3-propane diamine at 45°C for 3 h. The residue was dissolved in dichloromethane and washed with diethyl ether. Subsequently, the mixture of chlorambucil, benzotriazole-1-yl-oxy-tris-pyrrolidino-phosphonium hexafluorophosphate (PyBOP) and *N,N*-diisopropylethylamine (DIEA) in dimethylformamide (DMF) was added to the crude compound and stirred at room temperature for 1.5 h. After washing with diethyl ether, the crude was purified by HPLC to obtain the target product.

2.3 | Cellular viability assay

The cells were treated with or without etoposide (Tokyo Kasei Kogyo) or hydrogen peroxidase (Wako) with the indicated concentrations for an additional 2 days. The cells were washed with PBS once and calcein-AM (0.5 μM; Toyobo) was added for 30 min. The calcein fluorescence (Ex. 500 nm, Em. 520 nm) was detected using a microplate reader (Synergy H; Bio Teck) and the viability was calculated based on vehicle-treated cells (%).

2.4 | Gene set enrichment analysis

The microarray data from the NCBI GEO database under accession number (GSE130072) were reanalyzed using a different gene set with gene set enrichment analysis (GSEA) software as described previously. [22]

2.5 | Reverse transcription (RT) and real-time polymerase chain reaction (PCR)

Total RNA was subjected to RT with the use of ReverTra Ace with genome remover (Toyobo). The cDNA was subjected to real-time PCR analysis with LightCycler 96 (Roche) using the Thunderbird SYBR qPCR Mix (Toyobo) or Luna Universal qPCR Master Mix (NEB) as described previously.[18] All qPCR reactions were performed with RPS18 as an internal control. Primer sequences are listed in Table S1.

2.6 | Senescence-associated SA-β-gal assay

Cells were fixed and stained with S-β-gal using the SA-β-gal assay kit (Cell Signaling Technology) according to the manufacturer's protocol. Scales were 200 μm.

2.7 | Western blotting

Western blotting analysis was performed as described previously.[23] Primary antibodies were used as follows: p-mTOR(Ser2448) (D9C2; CST), p-mTOR(Ser2448) (D9C2; CST), β-actin (66009–1-Ig, Proteintech), mTOR (D9C2; CST), p-p70S6K(T389) (108D2;CST), p70S6K (49D7; CST), p-AKT(S473) (D9E; CST), AKT(pan) (C67E7; CST). The quantification of the band intensities was done using ImageStudio software (LI-COR Inc.).

2.8 | Annexin V apoptosis assay

The cells were washed with annexin V buffer (5 mM Ca^{2+}) and stained with annexin V-phycoerythrin (PE) (Biolegend) or annexin V-biotin (Biolegend) for 30 min at RT. For the staining with annexin V-biotin, cells were then washed with annexin V buffer and Cy3-streptavidin (Biolegend) was added for an additional 30 min. After washing, the cells were analyzed with BZ-X800 (Keyence). Scales were 100 μm.

2.9 | Phospho-γH2AX staining

Cells were fixed with 4% paraformaldehyde for 5 min, washed with PBS, and permeabilized with 0.5% Triton X-100 containing 1% FBS. The cells were then washed and incubated with anti-phospho-γH2AX antibody (Ser139) (Millipore) for 1 h. The cells were washed, and further stained with anti-mouse Alexa Fluor 488 antibody (Thermo Fisher). After washing, the cells were incubated and stained with Hoechst 33258 (Dojinjo) for 5 min and fluorescence analyzed using a BZ-X800 instrument (Keyence). Scales were 100 μm.

2.10 | Caspase3/7 activity assay

The cells were incubated with etoposide for an additional 20 h before being analyzed using the caspase-Glo 3/7 assay (Promega), as described by the manufacturer. The luminescence measurement was normalized by the relative cell number measured by a replicate sample using resazurin fluorescence (λ_{ex} = 560 nm and λ_{em} = 590 nm Synergy H, Bio Teck). The median effective concentration (EC_{50}) for caspase activity was calculated by sigmoidal, 4PL regression using GraphPad Prism 9.

2.11 | Statistical analysis

No statistical methods were used to predetermine sample size. Experiments were not randomized, and investigators were not blinded to allocation during experiments. Statistical analyses were done using the two-tailed unpaired Student's *t*-test, or Welch's *t*-test for unequal variance for comparisons between two groups. Analyses were performed by one-way analysis of variance (ANOVA), two-way

ANOVA, or two-way ANOVA followed by the Dunnett post-hoc test, Sidak post-hoc test, or the Holm–Bonferroni method for multiple group comparisons using Microsoft Excel or GraphPad Prism 9. Differences were considered as significant based on a *p*-value of <0.05, unless otherwise stated.

3 | RESULTS

3.1 | PRCC-TFE3 upregulates HMOX1 expression and confers chemoresistance

We previously generated an Xp11.2 translocation RCC mouse model in which human PRCC-TFE3 transgene was expressed in mouse kidneys and reported that the *Ret* signaling pathway was enriched in these mouse kidneys.[18] To identify additional signatures enriched in response to PRCC-TFE3 expression in the Xp11.2 tRCC mouse kidneys, we performed GSEA using the hallmark gene sets from the Molecular Signatures Database (MSigDB).[22] This analysis revealed several notable signaling pathways that were highly enriched in the TFE3-RCC mouse kidneys including pathways involved in inflammation, innate immunity, cell cycle, apoptosis, hypoxia and mTORC1 signaling (Figure S1 and Figure 1A). Importantly, the enrichment of signatures related to inflammation, hypoxia, mTOR signaling, and apoptosis was also observed in the human Xp11.2 translocation RCC clinical samples.[9] MiT family genes including *TFE3* and *TFEB* have been associated with stress response functions. Recently, it was shown that TFE3 and TFEB modulated p53 dependent apoptosis pathways in response to DNA damage.[17] Thus, the MiT family gene transcription factors are thought to be associated with the control of expression of genes that respond to stress; however, the significance of their role as mediators of stress responsive pathways in TFE3-RCC is not well understood. We hypothesized that the enrichment for an apoptotic signature indicates higher expression of apoptotic mediators, which can make tumor cells resistant to various stresses that lead to apoptosis and contribute to cancer cell survival. To test this possibility, we first established an HK2 cell system (cell line established from human proximal tubules) that could express PRCC-TFE3 in a doxycycline-dependent manner, and treated the cells with etoposide or hydrogen peroxidase in

order to examine the cytotoxic effect of these cell stress-inducing reagents (Figure 1B,C). HK2 cells treated with either reagent exhibited cell death, whereas expression of PRCC-TFE3 before introducing these stress agents resulted in increased HK2 cell viability by 40% (etoposide) and 25% (hydrogen peroxidase), respectively (Figure 1C). These results suggested that HK2 cells in which PRCC-TFE3 was expressed acquired resistance to etoposide- and hydrogen peroxidase-induced cytotoxicity.

Next, we asked how cells expressing PRCC-TFE3 acquired chemoresistance. Etoposide and hydrogen peroxidase both induced cellular apoptosis that was mediated by the p53 pathway. Therefore, we evaluated GSEA hallmark genes for apoptosis and p53 pathways and identified 11 genes in common that were associated with both signatures (Figure 1D). These genes are known to have functions in accelerating apoptosis (*CASP1*, *ATF3*, *JUN*, *DDIT3*), cell-cycle regulation (*CDKN1A*, *CCND2*), oxidative stress response (*HMOX1*), and others (*F2R*, *BMP2*, *TAP1*) (Figure 1D). *CDKN1A* (p21*)* has been reported as a direct target transcript of TFE3 fusion proteins.[24] *HMOX1* (heme oxygenase1) has multiple roles in controlling cellular oxidative stress, metabolism, autophagy, and inflammation, and mediates cellular processes for cell survival against various stresses.[25] In addition, HMOX1 expression was shown to be involved in chemoresistance in tumor cells.[26,27] We confirmed that *HMOX1* mRNA expression was increased upon doxycycline-dependent PRCC-TFE3 induction in HK2 and HEK293 cell lines, suggesting that PRCC-TFE3 may control HMOX1 expression in TFE3-RCC (Figure 1E). Furthermore, we found that *HMOX1* mRNA was highly expressed in human TFE3-RCC samples (*n* = 11) included in The Cancer Genome Atlas (TCGA) data set, as well as *GPNMB* and *Hexokinase2* (*HK2*), the transcriptional target genes of PRCC-TFE3 (Figure S2). Therefore, we focused on addressing the hypothesis that the PRCC-TFE3/HMOX1 axis controlled cellular survival in TFE3-RCC.

To examine if PRCC-TFE3 controlled *HMOX1* transcription in TFE3-RCC cells, we performed shRNA-mediated PRCC-TFE3 knockdown in UOK120 and UOK124 cell lines, which are derived from human Xp11.2 translocation RCC with PRCC-TFE3 fusions. Knockdown of PRCC-TFE3 expression reduced the HMOX1 expression by 40%–50% in UOK120 and UOK124 cells (Figure 1F), indicating that PRCC-TFE3 controlled *HMOX1* transcription. We also tested the effect of PRCC-TFE3 or HMOX1 inhibition on

FIGURE 1 PRCC-TFE3 confers resistance to genotoxic reagents through HMOX1. (A) GSEA plot of differentially expressed genes comparing PRCC-TFE3 expressing kidneys (Cre⁺) and control kidneys (Cre⁻) demonstrates significant enrichment in apoptosis and p53 pathway signatures. FDR-*q*, false discovery rate *q*-value; NES, normalized enrichment score. (B) Schematic diagram showing the HK2 or 293 cells system expressing *PRCC-TFE3* in a doxycycline (dox)-inducible manner. (C) Cellular viability was measured with calcein-AM on *PRCC-TFE3* dox-inducible cells treated with etoposide or hydrogen peroxidase for 24 h (*n* = 3). (D) List of the genes as a core enrichment, which were commonly identified in both signatures in (A). (E) RT-qPCR analysis of *HMOX1* mRNA in HK2 or 293 cells with or without doxycycline treatment for 48 h (*n* = 3). (F) RT-qPCR analysis of *PRCC-TFE3*, *GPNMB*, and *HMOX1* in the patient-derived *PRCC-TFE3* RCC cell lines (UOK120, UOK124) with *PRCC-TFE3* knockdown (*n* = 3). (G, H) Cellular viability assay using calcein-AM on UOK120 and UOK124 cells in (F) treated with etoposide in (G) or peroxidase in (H) for 48 h (*n* = 3). (I) RT-qPCR analysis of *HMOX1* mRNA in UOK124 cells stably expressing shRNA targeting *HMOX1*. (J) Cellular viability assay using calcein-AM on UOK124 cells in (I). treated with etoposide or peroxidase for 48 h (*n* = 3). Data are means ± SD. **p* < 0.05, ***p* < 0.01 (the unpaired two-tailed Student's *t*-test, or Welch's *t*-test, two-way ANOVA, two-way ANOVA followed by the Sidak post-hoc test)
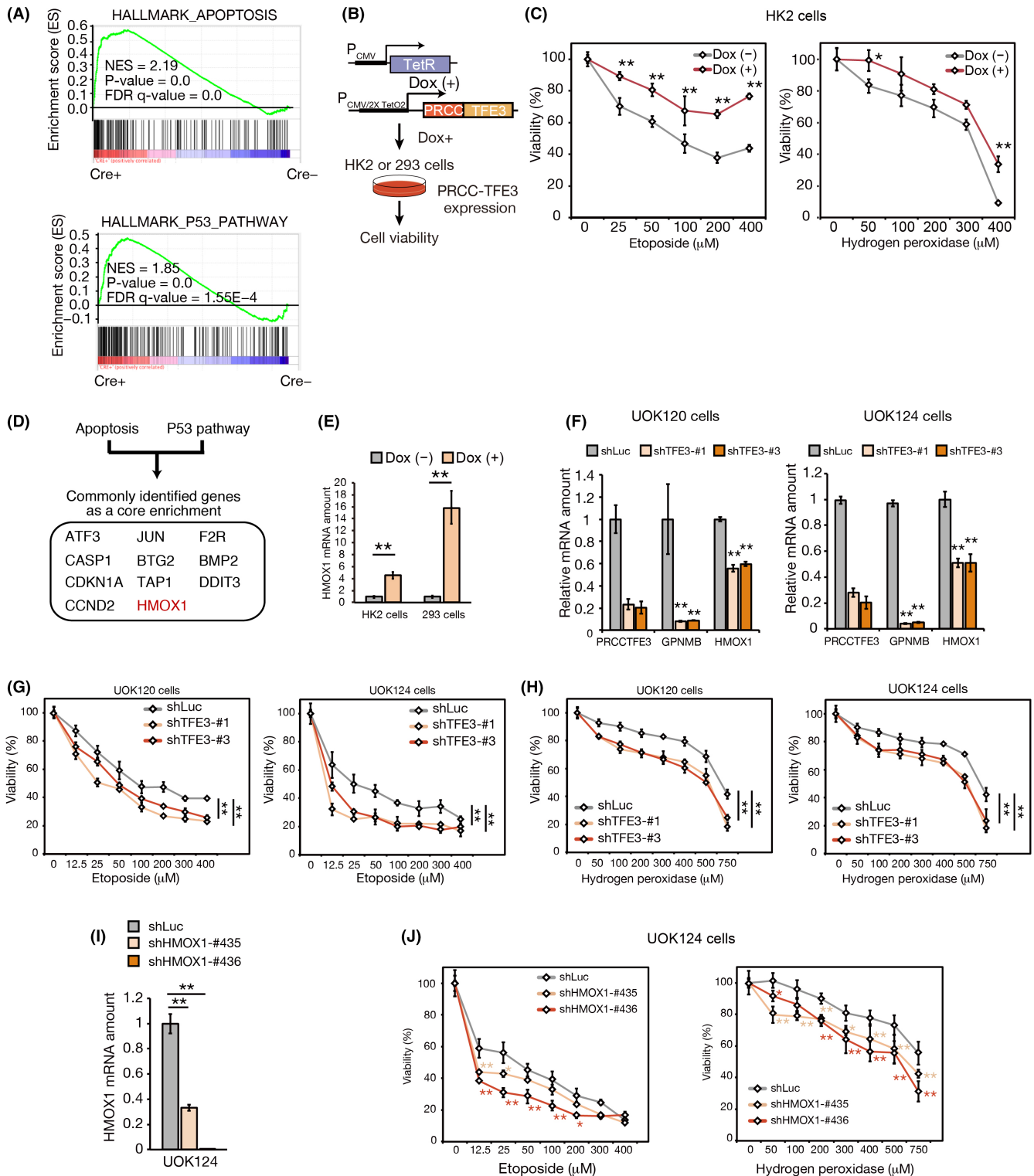
chemoresistance in UOK120 and UOK124 cells. Etoposide treatment of both cell lines showed a reduced viability; however PRCC-TFE3 knockdown further enhanced the cytotoxicity (Figure 1G). Similar results were observed in both UOK cell lines with hydrogen peroxidase (Figure 1H). Therefore, our results suggested that PRCC-TFE3 expression was responsible for chemoresistance in TFE3-RCC cells. Finally, to validate that the acquired chemoresistance was

dependent on HMOX1 in UOK120 and UOK124 cells, we knocked down *HMOX1* and repeated the same experiments (Figure 1I,J). These results confirmed that *HMOX1* knockdown also enhanced cytotoxicity to etoposide and hydrogen peroxidase in both UOK cells (Figure 1I). Overall, our data suggested that Xp11.2 translocation RCC (tRCC) cells show chemoresistance that was mediated by the PRCC-TFE3/HMOX1 axis.

3.2 | Identification of chlorambucil-conjugated PI polyamide (Chb16) for targeting TFE3 transcription

Clinically, most of the Xp11.2 translocation RCC tumors demonstrated strong nuclear TFE3 staining, suggesting that chimeric TFE3 proteins are constitutively activated in TFE3-RCC.[6,9] We hypothesized that inhibition of chimeric TFE3 transcriptional activity, which blocks the proposed acquisition of chemoresistance through the PRCC–TFE3/HMOX1 axis, might be an effective therapeutic strategy for TFE3-RCC. PI polyamides are synthetic oligomers that can recognize specific DNA sequences by designing the PI pairs to the target site of the genome.[28,29] Using the PI pairs targeting RUNX-binding sequences conjugated to the nitrogen mustard alkylating agent, chlorambucil (Chb), we previously showed that Chb can efficiently inhibit the recruitment of RUNX family transcription factors to their binding sites and demonstrated their therapeutic potential for acute myeloid leukemia (AML) cells.[21] We sought to take advantage of this technology to target the putative binding motifs of TFE3, and synthesized several Chb compounds harboring the PI pairs targeting putative TFE3 consensus sequences including TCAYRTG and CAYRTGA (Figure S3A and Figure 2A). All the Chb compounds were synthesized and purified using HPLC and the quality was confirmed using matrix-assisted laser desorption/ionization-time of flight mass spectrometry (MALDI-TOF/MS) (Figure 2B). We treated HK2 cells that expressed PRCC-TFE3 with these Chb compounds to test the inhibitory effect on the expression of GPNMB (glycoprotein nonmetastatic B), a well known direct transcriptional target gene of PRCC-TFE3 (Figure S3B). Treatment with Chb1 or Chb36 had only marginal or no inhibitory effect on GPNMB transcription upon PRCC-TFE3 expression (Figure S3B). Chb8 and Chb16 both produced an inhibitory response at a higher dose, but only Chb16 showed a dose-dependent inhibitory effect on the expression of GPNMB (Figure S3B). Thus, we focused on Chb16 and further confirmed the inhibitory effect of Chb16 on GPNMB mRNA in HK2 cells and also HEK293 cells expressing doxycycline-dependent PRCC-TFE3 (Figure 2C). We also validated the ability of Chb16 to inhibit another PRCC-TFE3 transcriptional target, HK2 (hexokinase 2) (Figure 2D).[30] TFE3-RCC is frequently observed to have activated mTOR signaling, which has been recently discussed as a potential therapeutic target for TFE3-RCC.[31] As expected, PRCC-TFE3 induction increased mTOR phosphorylation at Ser2448, and Chb16 was able to reduce the increased mTOR phosphorylation in a dose-dependent manner (Figure 2E). The well known mTOR downstream phosphorylation of AKT at Ser473,and p70 S6K at Thr389 also showed a similar response in a dose-dependent manner (Figure 2E). These results suggest that Chb16 may be effective in reducing mTOR activity in Xp11.2 tRCC tumor cells. Last, we confirmed that Chb16 inhibits the expression of HMOX1, which is upregulated by PRCC-TFE3 transcription (Figure 2F). Overall, these results suggested that Chb16 is effective in inhibiting the expression of multiple genes induced by PRCC-TFE3 transcription, and may also be useful to control the target gene expressions in TFE3-RCC.

3.3 | Chb16 induces cell-cycle arrest at G2/M in PRCC-TFE3 RCC cells

Next, we attempted to characterize how Chb16 exhibits its effect on the Xp11.2 tRCC cells that express PRCC-TFE3 using the patient-derived TFE3-RCC cell lines, UOK120, UOK124, and UOK146. Chb16 treatment of the TFE3-RCC cell lines clearly showed reduced cell proliferation in a dose-dependent manner (Figure 3A). Growth inhibition was accompanied by cellular morphological changes toward a more spreading, spindle-like shape (Figure 3B). We examined whether the growth inhibition and morphological changes were caused by apoptotic cell death by staining with annexin V (Figure 3C). We found no significant increase in annexin V-positive cells after Chb16 treatment, suggesting that the Chb16-treated cells were not dying through apoptosis (Figure 3C). In order to determine how cells were exhibiting growth arrest, we examined the cell cycle by BrdU incorporation and DNA staining. Chb16-treated cells had a significant increase in the G2/M phase in all Xp11.2 tRCC cell lines (Figure 3D–F). Collectively, these data indicated that Chb16 treatment induced cell-cycle arrest at the G2/M phase in tRCC cells, but was not accompanied by apoptotic cell death.

3.4 | Induction of the DNA damage response by Chb16 in PRCC-TFE3 cell lines

Next, we asked how growth arrest at G2/M in tRCC cells occurred following Chb16 treatment. At the G2/M phase transition, cells undergo a mitotic checkpoint to ensure that they have error-free copies of DNA. Upon encountering DNA damage, cells stop at the G2/M checkpoint and correct the error to prevent its inheritance by the daughter cells, or they initiate the apoptotic process.[32] It is commonly understood that DNA stress including inducers of physical damage (UV, irradiation, and hydrogen peroxidase), as well as commonly used cancer drugs (etoposide, cisplatin, etc.) may all act to initiate G2/M cell-cycle arrest, but when the damage is too severe to recover, the cells will undergo apoptosis. We hypothesized that the Chb16 effect on tRCC cells leading to the G2/M arrest is caused by activation of the DNA stress pathway. To test this possibility, we stained Chb16-treated TFE3-RCC cells with phospho-γH2AX and, indeed, found that Chb16 treatment showed an increase in phospho-γH2AX-positive cells, albeit with a milder effect compared with hydrogen peroxidase (Figure 4A,B). Compared with hydrogen peroxidase, which is a ROS generator that leads to a strong response to DNA damage, Chb16 is a relatively mild DNA stress inducer in TFE3-RCC cells.

The p53 pathway integrates stress responses, and initiates transcriptional programs that govern diverse processes involving DNA repair, cell-cycle arrest, and apoptosis when cellular damage is too strong to recover.[33] We checked the mRNA expression levels of p53 and its transcripts that are normally upregulated in apoptosis (Figure 4C). Chb16 treatment increased p21 mRNA expression very strongly in a time-dependent manner, but expression levels of other p53 target genes including BAX and
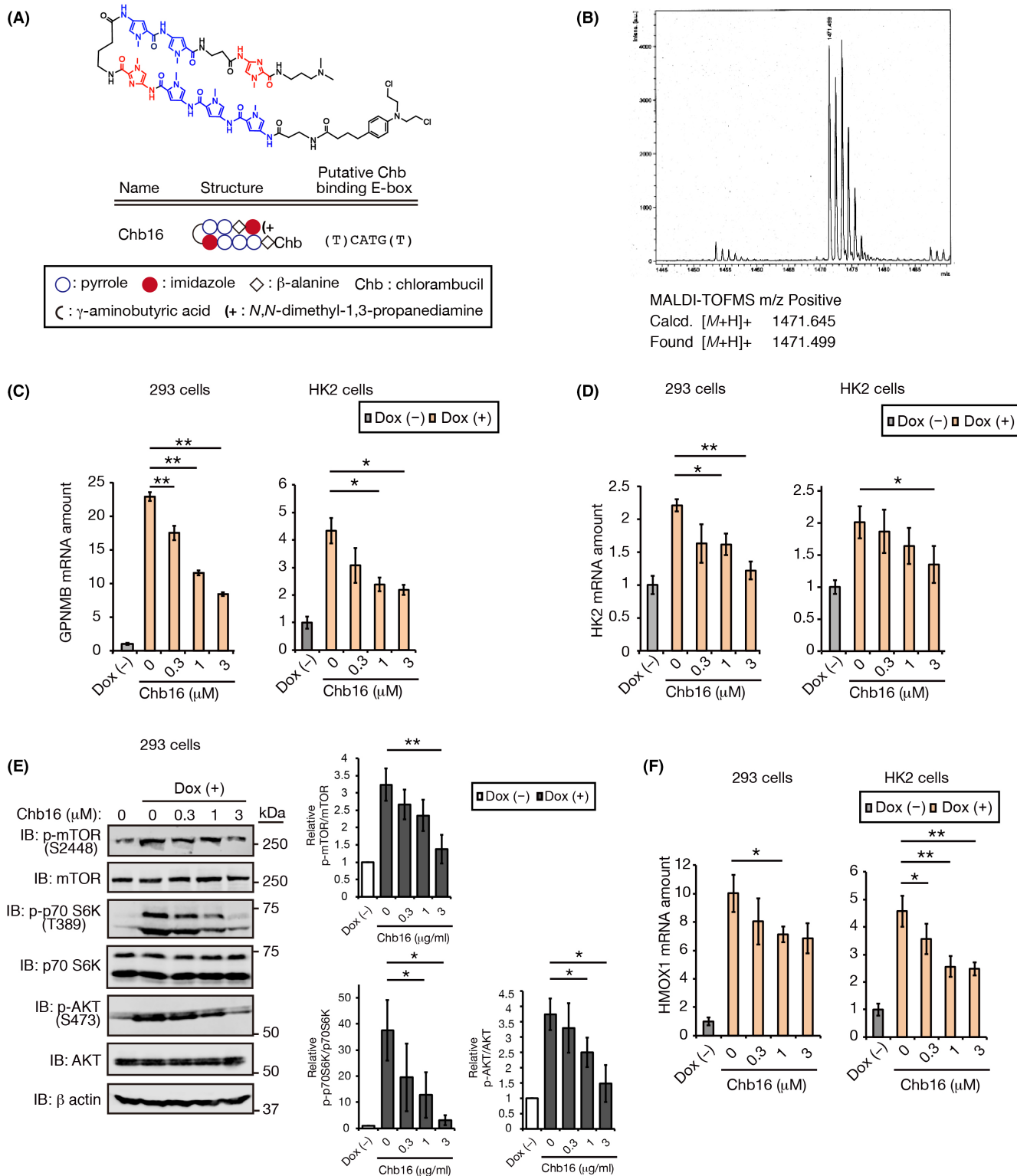
FIGURE 2 Identification of Chlorambucil-conjugated PI polyamide (Chb16) for targeting TFE3 transcription. (A) Chemical structure of Chb16 and its putative DNA binding sequence. (B) MALDI-TOF MS spectrum of Chb16 which was purified by HPLC. (C, D) RT-qPCR analysis of PRCC-TFE3 target genes GPNMB (C) and hexokinase 2 (HK2) (D) on PRCC-TFE3 doxycycline-inducible HK2 or 293 cells with Chb16 treatment in a dose-dependent manner ($n = 3$). (E) Western blotting analysis (left panel) of phospho-mTOR (ser2448), phospho-p70 S6K (Thr389), and pAKT(S473) on PRCC-TFE3 doxycycline-inducible 293 cells. Cells were pretreated with different dosages of Chb16 prior to doxycycline induction for 24 h. β-Actin serves as a loading control. Quantification of western blot band intensities (right panels, $n = 3$). (F) RT-qPCR analysis of *HMOX1* as in (C) ($n = 3$). Data are means ± SD. *$p < 0.05$, **$p < 0.01$ (the unpaired two-tailed Student's *t*-test, or Welch's *t*-test corrected by the Holm–Bonferroni method for multiple comparisons)

PUMA were upregulated but to a lesser extent (Figure 4C). No change in *p53* mRNA expression itself was observed (Figure 4C). These results are consistent with a milder effect of Chb16 on DNA damaging responses. Taken together, we conclude that Chb16 treatment leads to a weak DNA damage response in tRCC cells, which may be mediated by the p21-dependent pathway leading to growth arrest.

3.5 | Chb16 induces cellular senescence in PRCC-TFE3 cell lines

Growth arrest at the G2/M checkpoint can be transient, but also leads cells to stop terminal cellular proliferation through senescence. Given that the Chb16-treated cells changed morphology to a spreading, spindle-like transitional shape, a morphological phenotype reminiscent of senescence (Figure 3B), we speculated that a prolonged treatment with Chb16 may also induce terminal proliferation arrest in TFE3-RCC cells by undergoing cellular senescence. Indeed, PRCC-TFE3 cells treated with Chb16 for 4 days showed an increased number of senescence-associated beta-galactosidase (SA-β-gal) positive cells, which increased in a Chb16 dose-dependent manner (Figure 5A,B). *Lamin B1* loss is another marker for cells undergoing cellular senescence,[34] and consistently Chb16-treated cells showed reduced *lamin B1* mRNA expression in a time-dependent manner (Figure 5C). The senescent phenotype is not limited to an arrest of cell proliferation but is often associated with widespread expression and secretion of inflammatory proteins, which is known as the SASP.[35] We thus checked expression levels of the SASP-related genes (*IL-1β*, *IL6*, and *IL8*) and confirmed increased expressions in response to Chb16 treatment in TFE3-RCC cells (Figure 5D). Taken together, these data suggested that growth arrest by a prolonged Chb16 treatment in UOK cells expressing PRCC-TFE3 is accompanied by cellular senescence, which appears to cause morphological changes as well.

3.6 | Chb16-induced cellular senescence is dependent on p21 pathway and contributes to reduced proliferation

We next asked whether senescence following Chb16 treatment is responsible for the reduced cell proliferation. While various upstream

pathways are known to mediate an induction of senescence accompanied by the DNA damage response, p53 and p21 often play critical roles in controlling the senescence-associated phenotypes. During the DNA damage response p53 activity controls p21 to activate downstream pathways.[36] Given that *p21* mRNA is notably expressed in response to Chb16 treatment (Figure 4C), we hypothesized that increased p21 expression or p53 activity that controls p21 is responsible for the Chb16-induced cellular senescence and subsequent proliferation arrest.

To test this possibility, we first knocked down *p53* or *p21* in UOK124 and UOK146 cells using an infection of lentivirus containing shp53 or shp21 (Figure 6A), and treated the cells with Chb16. In both cases, Chb16-treated TFE3-RCC cells with p53 or p21 expression had more SA-β-gal-positive cells than the untreated cells, whereas Chb16 treatment of *p53* or *p21*-knockdown TFE3-RCC cells resulted in a greater number of SA-β-gal-positive cells, but not to the level seen in Chb16-treated p53 or p21 expressing cells, suggesting that both p53 and p21 pathways are partially involved in Chb16-induced senescence (Figure 6B,C). We also tested the knockdown effect on cellular proliferation. While p53 knockdown has a minimal effect on proliferation arrest, p21 knockdown partially rescued the proliferation arrest in TFE3-RCC cells (Figure 6D). These data consistently show that the *p21* mRNA is upregulated more significantly after Chb16 treatment than p53 mRNA. Thus, Chb16-induced proliferation arrest depends more on p21 expression than on p53, and p21 is partially responsible for the efficient induction of the Chb16-induced proliferation arrest.

3.7 | Combined treatment of Chb16 with etoposide sensitized tRCC cells for apoptosis

Chemoresistance that involves the PRCC-TFE3/HMOX1 axis would predict that inhibition of this axis combined with commonly used cancer drugs may give Xp11.2 tRCC cells more vulnerability. Etoposide is a widely used cancer drug used also in RCC chemotherapy that causes cellular apoptosis through topoisomerase II inhibition, thereby inducing DNA stress.[37] We reasoned that Chb16 treatment to inhibit PRCC-TFE3 transcription and induce mild DNA stress may augment the efficacy of etoposide-induced apoptosis in tRCC cells. To validate this argument, we first treated tRCC cells with etoposide following treatment with a gradient

FIGURE 3 Chb16 induces proliferation arrest at G2/M in PRCC-TFE3 RCC cell lines. (A) Cell proliferation curves of PRCC-TFE3 RCC cells treated with the different dosages of Chb16 (*n* = 3). (B), Representative pictures of UOK124 cells treated with Chb16 for 3 days. Scale bars, 200 μm. Inset scale bar, 50 μm. (C) Annexin V staining of UOK124 cells with Chb16 treatment for 24 h (left panel). Etoposide (ETP)-treated cells serve as an apoptotic cell control. Merged images in which nuclei are stained with Hoechst 33258 are also shown. Scale bars, 50 μm. Number of annexin V-positive cells (%) are shown (right panel; *n* = 3). (D) Cell-cycle analysis of UOK120 cells treated with Chb16 (1 μM) for 24 h. Cells were labeled with BrdU for 90 min, fixed, and stained with phycoerythrin (PE)–conjugated antibodies to BrdU. Nuclear DNA was stained with 7-AAD, and the cells were then analyzed by flow cytometry. Representative flow cytometric analysis is shown on the left (top: control; bottom: Chb16 (1 μM)), and its relative cell-cycle phases were shown on the right (*n* = 3). (E, F) Cell-cycle analysis of UOK124 cells (E) and UOK146 cells (F) in experiments similar to that shown in (D). Data are means ± SD. *p < 0.05, **p < 0.01; ns, not significant (two-way ANOVA followed by the Dunnett post-hoc test, one-way ANOVA)

(A)

(B)

(C)

(D)

(E)

(F)
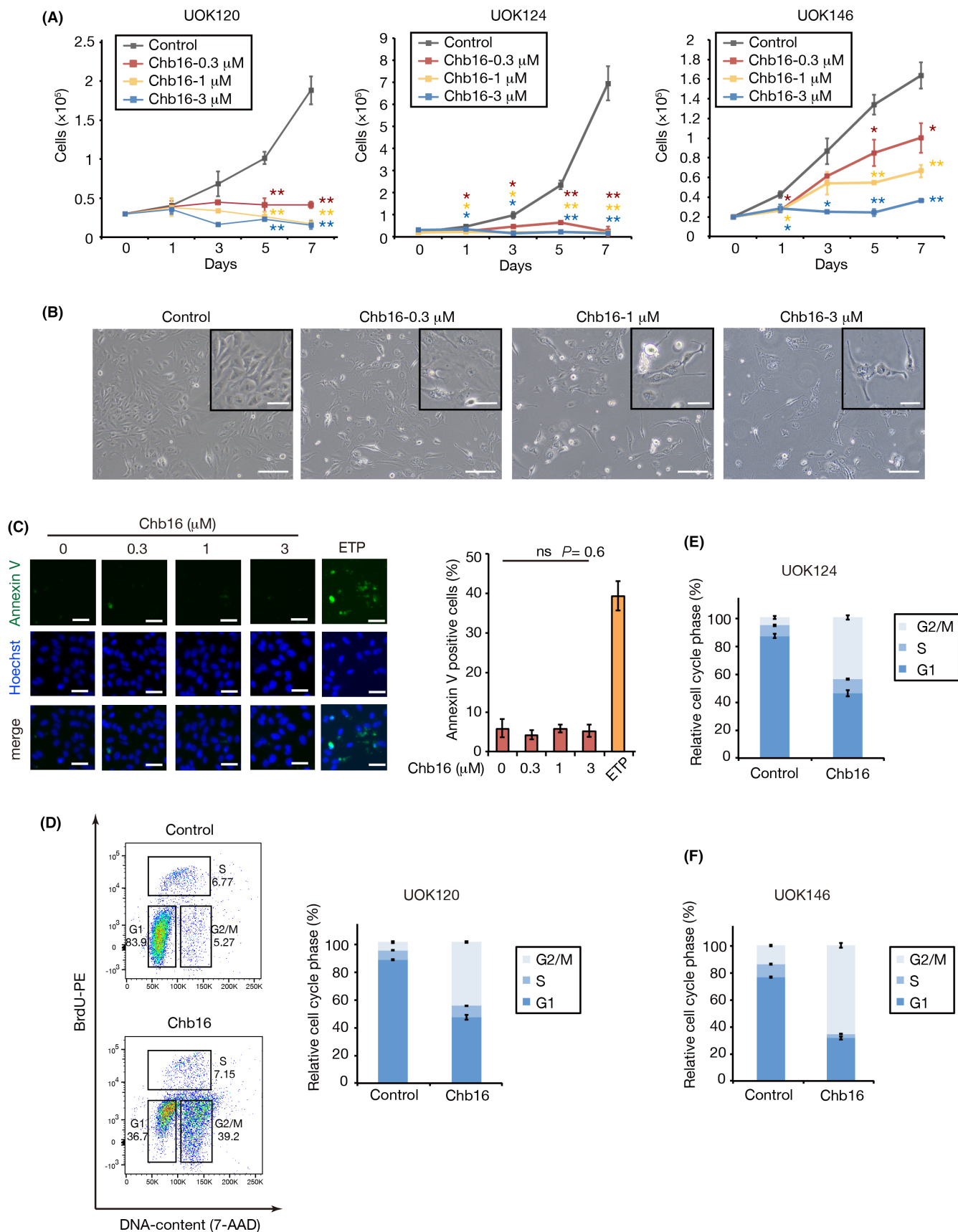
dose of Chb16 for 24 h. Interestingly, while Chb16 treatment alone did not induce apoptosis, the combined treatment of etoposide with Chb16 increased the number of apoptotic cells in a Chb16 dose-dependent manner (Figure 7A). Thus, our data suggested that Chb16 enhanced etoposide-induced apoptosis in tRCC cells. Next, we sought to test if this Chb16 effect is observed in other

cell types that have no PRCC-TFE3 expression. We tested the combined treatment of Chb16 in renal cell lines without *PRCC-TFE3* translocation (HK2 and 786-O) and interestingly found that Chb16 has no additional effects on etoposide-induced apoptosis in these cells (Figure 7B,C). Notably, etoposide-induced apoptosis more efficiently in non-TFE3-RCC, renal tubule derived cells in the absence of Chb16 treatment, which was not further enhanced by Chb16 (Figure 7B,C), indicating that renal cells without PRCC-TFE3 are more sensitive to the cancer drug. Consistently, a knockdown of PRCC-TFE3 mRNA in TFE3-RCC cells showed much more efficient apoptosis induction by etoposide, similar to the level seen in the non-tRCC cells (Figure 7D). In PRCC-TFE3 RCC, pre-treatment of Chb16 together with etoposide

augmented apoptosis to the same extent as in PRCC-TFE3 knockdown cells (Figure 7D). We further confirmed a similar effect on the caspase 3/7 activity in UOK120 cells (Figure 7E). Consistent with annexin V results in Figure 7D, etoposide-induced caspase 3/7 activity was enhanced with Chb16 by 2.5-fold (EC_{50} for ETP is 15.3 μM versus EC_{50} for ETP +Chb16 is 6.15 μM) in UOK120 cells (Figure 7E). Knockdown of PRCC-TFE3 also demonstrated the enhancement of caspase 3/7 activation by ETP to an extent similar to Chb16 treatment (EC_{50} for ETP is 3.74 μM) (Figure 7E). Furthermore, Chb16 treatment did not show enhancement of caspase 3/7 activity in TFE3 knockdown UOK120 cells (EC_{50} for ETP + Chb16 is 5.22 μM). Caspase 3/7 activity was not increased by Chb16 treatment alone even at a high concentration (Figure S4).

FIGURE 4 Induction of DNA damage responses by Chb16 in PRCC-TFE3 RCC cell lines. (A, B) UOK120 cells (A) or UOK124 cells (B) treated with Chb16 (1 μM) or hydrogen peroxidase (500 μM, positive control) were immunostained with anti-phospho-γH2AX antibodies. Representative merged images in which nuclei were stained with Hoechst 33258 are also shown (left panel). Scale bars, 100 μm. The percentage of phospho-γ-H2AX-positive cells was calculated (right panel, *n* = 3). (C) Expression of p53 downstream genes was analyzed by RT-qPCR in PRCC-TFE3 RCC cell lines after treatment with Chb16 (1 μM) for the indicated time course (*n* = 3). Data are means ± SD. *$p < 0.05$, **$p < 0.01$ (Welch's *t*-test corrected by the Holm–Bonferroni method for multiple comparisons)
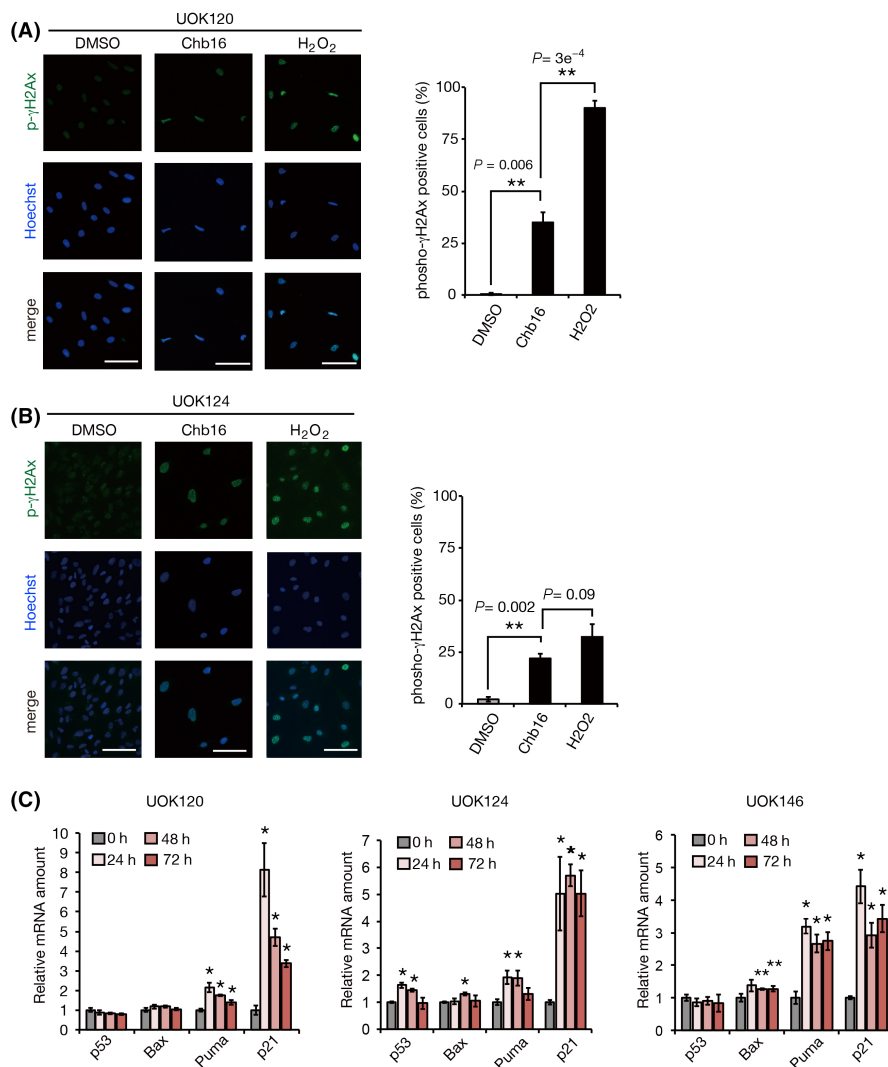
FIGURE 5 Chb16 induces cellular senescence in PRCC-TFE3 RCC cells. (A, B) Three different PRCC-TFE3 RCC cell lines UOK120, UOK124, and UOK146 were treated with indicated concentrations of Chb16 for 4 days and stained for SA-β-gal activity (blue). The representative microscopy images are shown in (A). The bright field images were used for determination of the proportion of senescent cells in (B). Scale bars, 100 μm. (C) RT-qPCR analysis of laminB1 mRNA was analyzed in PRCC-TFE3 RCC cells after treatment with Chb16 (1 μM) for the indicated time course (*n* = 3). (D) RT-qPCR analysis of SASP factor mRNAs was analyzed as in (C). Data are means ± SD. *$p < 0.05$, **$p < 0.01$ (the Welch's *t*-test corrected by the Holm–Bonferroni method for multiple comparisons)
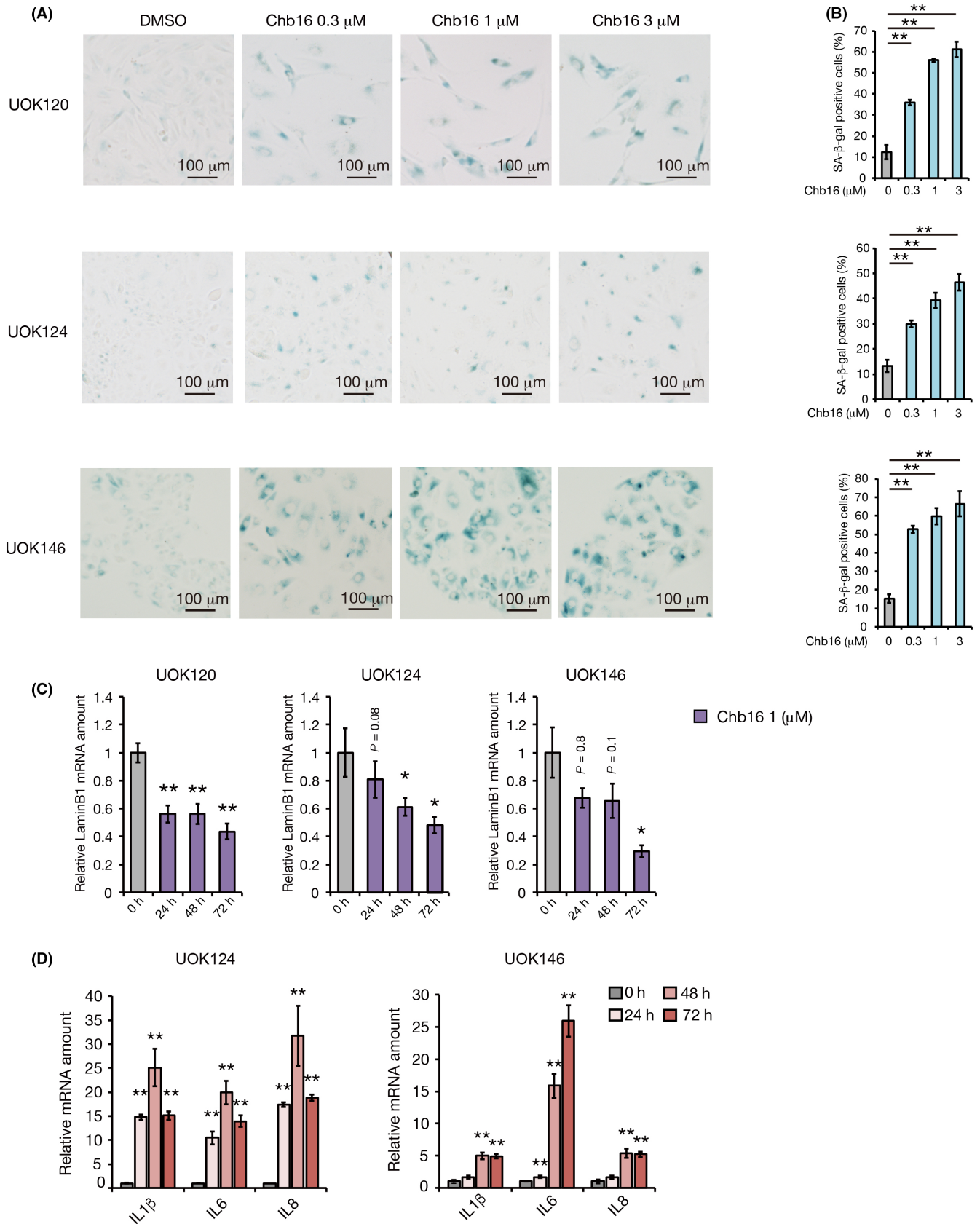
These results confirmed that Chb16 enhanced etoposide-induced apoptosis in TFE3-RCC cells, and this augmentative effect relied on PRCC-TFE3 expression.

Overall, we have shown that the PRCC-TFE3 transcription plays a role in conferring chemoresistance through the expression of genes such as HMOX1. A novel PRCC-TFE3 transcriptional

inhibitor Chb16 acts by two mechanisms on TFE3-RCC cells. First, inhibition of the PRCC–TFE3/HMOX1 axis reduced the acquired chemoresistance. Chb16 treatment alone also shows proliferation arrest on TFE3-RCC cell lines, which is based on mild DNA stress activation and cellular senescence (Figure 7F). Treatment

with Chb16 together with a genotoxic cancer drug augmented the accumulation of DNA damage from the Chb16 stress, while it also directly sensitized cells to apoptosis through inhibition of the PRCC–TFE3/HMOX1 axis (Figure 7F). By taking advantage of these mechanisms, Chb16 might be used in combination with a
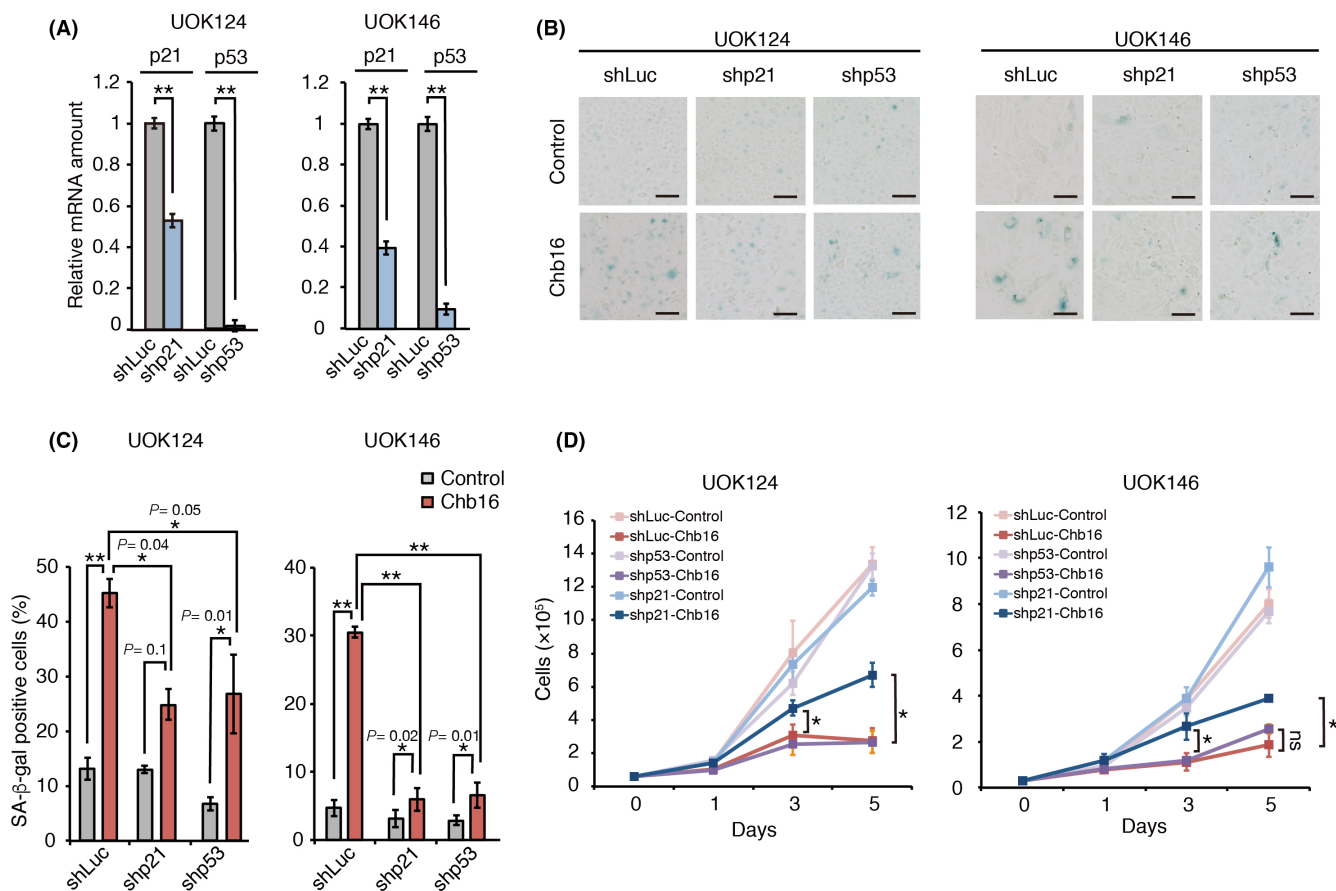

FIGURE 6 Chb16-induced cellular senescence is dependent on p21 pathway in PRCC-TFE3 RCC cells. (A) RT-qPCR analysis of *p21* or *p53* mRNA was analyzed in PRCC-TFE3 RCC cells stably expressing shRNA targeting luciferase (shLuc), *p21* (shp21) or *p53* (shp53). The shLuc serves as a non-target control (n = 3). (B) PRCC-TFE3 RCC cells stably expressing shLuc, shp21 and shp53 were treated with Chb16 (1 μM) for 4 days, and stained for SA-β-gal activity (blue). The representative images were observed by microscopy (A). Scale bar, 100 μm. (C) The percentage of senescent (SA-β-gal-positive) cells in each condition shown (B) was calculated (n = 3). (D) Growth curves of PRCC-TFE3 RCC cells stably expressing shRNA targeting luciferase (shLuc), *p21* (shp21) and *p53* (shp53) with or without Chb16 (1 μM) (n = 3). Data are means ± SD. *$p < 0.05$, **$p < 0.01$ (the unpaired two-tailed Student's *t*-test, two-way ANOVA followed by the Sidak post-hoc test)

FIGURE 7 Chb16 treatment abrogates PRCC-TFE3 dependent chemoresistance of PRCC-TFE3 RCC cells. (A) Annexin V staining analysis of UOK120 cells which were treated with indicated concentrations of Chb16 for 24 h, followed by etoposide treatment (ETP; 150 μM) for 24 h. Merged images in which nuclei are stained with Hoechst 33258 are also shown (left panel). Scale bars, 50 μm. Annexin V-positive cells (%) were counted (right panel) (n = 3). (B, C) Annexin V staining analysis of HK2 (B) and 786-O (C) cells which were treated with or without Chb16 (3 μM) for 24 h, followed by etoposide (ETP) treatment for 24 h. Merged images in which nuclei are stained with Hoechst 33258 are also shown (left panels). The annexin V-positive cells (%) were counted (right panels) (n = 3). (D) The same experiments shown in (B) and (C) were performed on stably expressing shTFE3 or control shLuc expressing UOK120 cells, which were treated with Chb16 (1 μM) for 24 h followed by etoposide treatment (ETP; 150 μM). Scale bars, 50 μm. Data are means ± SD. *$p < 0.05$, **$p < 0.01$; ns, not significant (two-way ANOVA followed by the Holm–Bonferroni post-hoc test). (E) Caspase 3/7 activity luminescence (RLC) was measured by caspase-Glo 3/7 assay, which was normalized by cell number (resazurin fluorescence: $\lambda_{ex} = 560$ nm and $\lambda_{em} = 590$ nm), (n = 3). The EC_{50} values were calculated by sigmoidal, 4PL regression analysis. (F) The proposed mechanism by which PRCC-TFE3 RCC cells acquire chemoresistance and the effect of Chb16. Briefly, PRCC-TFE3 confers chemoresistance through expression of downstream genes including *HMOX1*. Chb16 inhibits its transcription to reduce chemoresistance from genotoxic agents such as etoposide. Chb16 also exhibits DNA stress to enhance the cytotoxicity of a cancer drug such as etoposide

(A)

(B)

(C)

(D)

(E)

(F)
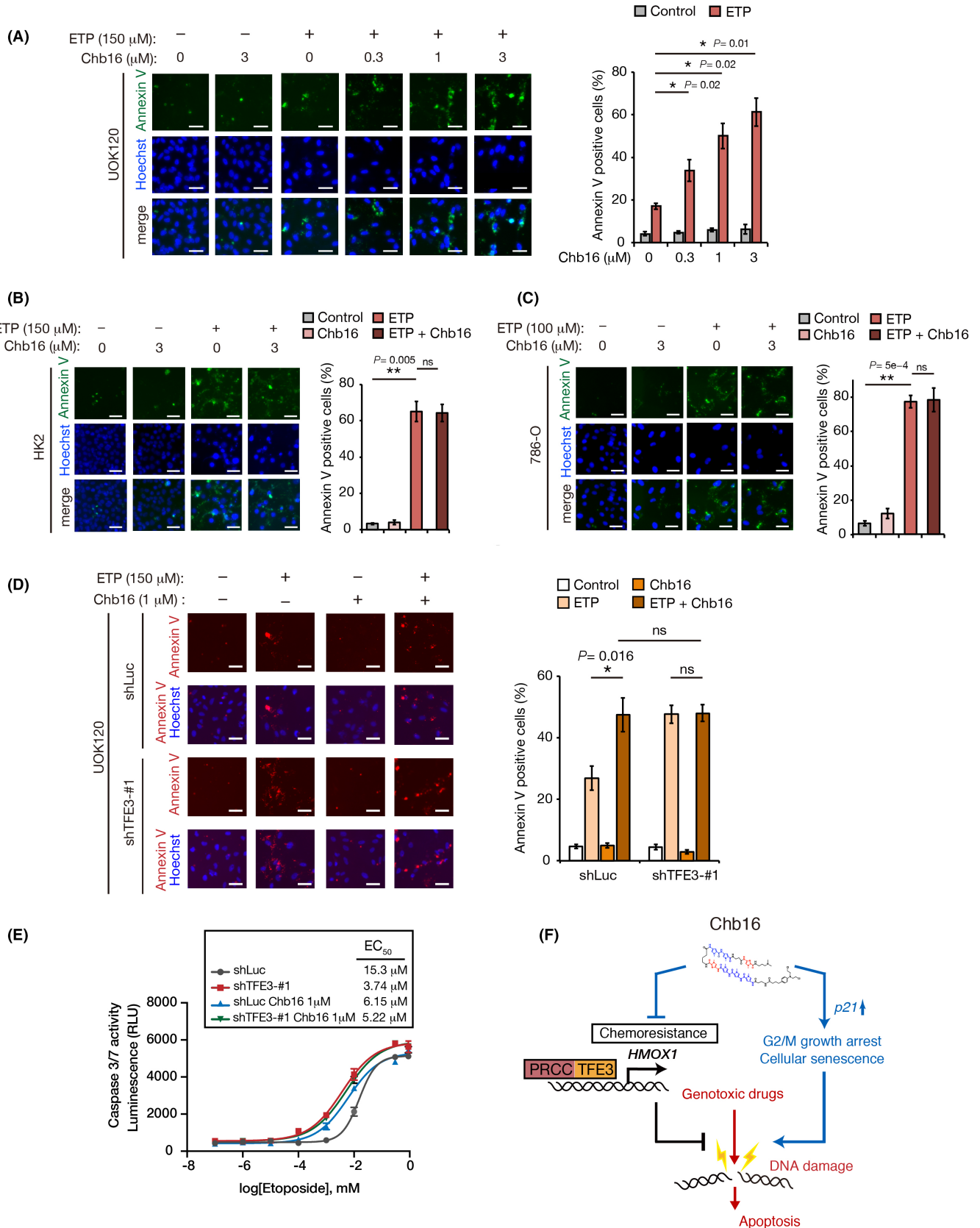
therapeutic agent such as etoposide to selectively target cancer cells for apoptosis, suggesting that such a combination of agents may provide a novel therapeutic approach for advanced forms of TFE3-RCC.

4 | DISCUSSION

The heterogeneous morphologies and limited availability of the Xp11.2 translocation RCC (TFE3-RCC) models hinders our

understanding of the characteristics of TFE3-RCC that contribute to tumorigenesis.[6] The findings reported here support a novel mechanism in which an oncogenic TFE3 fusion protein controls HMOX1 expression to confer chemoresistance in TFE3-RCC cells. In addition, we have identified a novel PRCC-TFE3 transcriptional inhibitor, Chb16, and demonstrated that Chb16 use can reduce acquired chemoresistance in PRCC-TFE3 expressing RCC cell lines. Combination treatment of Chb16 with etoposide enhanced the etoposide cytotoxicity, underscoring the importance of targeting the PRCC–TFE3/HMOX1 axis for maximum efficacy of the cancer drug. The finding that Chb16 treatment sensitized cells to etoposide highlights the potential of Chb16 combination chemotherapy for treating PRCC-TFE3 RCC.

Cancer chemoresistance is a serious challenge. Multiple intracellular mechanisms of chemoresistance have been identified in cancer, including multidrug transporters, oncogene activity, DNA repair, autophagy, epithelial–mesenchymal transition (EMT), and cancer stemness.[38,39] In the current study, we have confirmed that PRCC-TFE3 controls HMOX1 expression and shown that inhibition of the PRCC–TFE3/HMOX1 axis sensitizes cells to genotoxic stress caused by etoposide or hydrogen peroxidase in TFE3-RCC cell lines. HMOX1 was originally identified as an enzyme that catalyzes the rate-limiting step in heme biosynthesis.[40] HMOX1 also produces CO, ferrous ion, and biliverdin, all of which play a role in reducing oxidative stress and preventing cell apoptosis.[40] Consistently higher expression of HMOX1 has been reported in various types of cancer such as hepatoma, melanoma, renal cancer, and brain cancer.[41–44] Thus, HMOX1 function is not limited to its original biological role of catalyzing heme production but may have broader functions in mediating environmental stress for tumor cell survival and proliferation.

Activation of the NRF2 pathway, which detoxifies ROS stress is known to be an important mechanism to reduce ROS stress and damaged DNA in various types of tumor cells.[45] HMOX1 is one of the well known downstream genes that is directly controlled by the NRF2 pathway, acting as an antioxidative stress response gene.[46] Upregulated NRF2 transcription has been reported in a sporadic papillary RCC.[47] Notably, we found a potential upregulation of NRF2 in our transcriptome data from the PRCC-TFE3 expressing mouse kidneys.[18] It will be interesting to see whether HMOX1 expression by PRCC-TFE3 is also dependent on the NRF2 pathway. Additionally, MiT family proteins including TFEB and TFE3 have been previously shown to regulate stress responses by activating autophagy in response to ROS.[48–50] In a recent paper, PRCC-TFE3 RCC was found to be insensitive to killing by a mitochondrial ROS inducer through PRKN-dependent mitophagy.[51] The functional relevance of HMOX1 in reducing oxidative stress responses has not been well investigated in Xp11.2 translocation RCC tumor. Given that HMOX1 expression also participates in acquired resistance against hydrogen peroxidase treatment, HMOX1 expression in PRCC-TFE3 RCC may work more broadly against general environmental stress. Whether or not PRCC-TFE3 coordination with the stress response pathways contributes to tumor development *in vivo* needs further investigation.

Xp11.2 translocation RCC is known to be an aggressive malignancy with high rates of recurrence and metastasis.[52] Given the lack of effective forms of therapy, the standard chemotherapies for clear cell RCC are commonly used for advanced TFE3-RCC tumors; however they are often refractory.[53] Our results suggest that inhibition of the enhanced transcriptional activity of TFE3 fusion proteins could be a mechanism for reducing chemoresistance in TFE3-RCC which supports the development of potential inhibitors and their use in combination with current clinical therapies to increase sensitivity and efficacy for advanced TFE3-RCC patients.

We have approached the idea of targeting PRCC-TFE3 transcriptional activity by designing a chemical inhibitor that binds to TFE3 consensus sequences. The flat interaction surfaces of oligonucleotides and binding proteins often make it challenging to screen and design a synthetic chemical inhibitor for a transcriptional regulator that can bind to its consensus sequence on DNA.[54] Here, our approach was to design with PI-based Chb inhibitors that can target TFE3 binding sequences on DNA. One of the candidates from the group of designed chemical inhibitors, Chb16, showed inhibition of both GPNMB and HMOX1 expression induced by PRCC-TFE3 transcription. To our knowledge, Chb16 is the first potential inhibitor for TFE3 transcriptional targets.

We would predict that Chb16 binds preferentially to the MiT/TFE consensus sequences (TCATGTG or CACATGA), which may be found frequently in other regions of the genome besides PRCC-TFE3 target gene promoters. Treatment with Chb16 alone showed stronger proliferation arrest than was seen with PRCC-TFE3 mRNA knockdown in TFE3-RCC cells, suggesting that the proliferation arrest may be in part mediated through alternative mechanisms, possibly through Chb16 interaction with other regions. Consistent with this observation, Chb16 alone also induced a mild DNA damage response. This activation did not lead to p53-mediated apoptosis. Thus, Chb16 is not itself an inducer of apoptosis and is only responsible for G2/M arrest and potentially for cellular senescence. These kinds of off-target effects may cause side effects in patients treated with Chb16 alone or in combination with genotoxic chemotherapeutics. Chb16 also inhibits physiological gene expression by endogenous MiT/TFE transcription factors in normal cells, which may also cause adverse effects in patients. Further work to evaluate the contribution of potential Chb16 off-target binding would be necessary to identify and minimize the side effects of Chb16 treatment in a clinical setting.

To demonstrate an effective therapeutic strategy using Chb16 in combination with a currently available cancer drug, we tested Chb16 with etoposide to induce apoptosis in TFE3-RCC cells. Notably, Chb16 treatment enhanced the cytotoxicity of etoposide in a PRCC-TFE3-dependent manner. Chb16 alone did not induce apoptosis even at high concentration. Therefore, Chb16 is synergistic only when used in combination with etoposide where it increases cytotoxicity in PRCC-TFE3 expressing TFE3-RCC cells. p21 is the essential downstream effector for apoptosis in the p53 pathway. Chb16 treatment in PRCC-TFE3 RCC cells upregulated p21 mRNA expression at high level. Thus, the etoposide-induced apoptosis may also be augmented through increased activity of p53 downstream mechanisms, of which p21 may be an important mediator. Using a

combination strategy to selectively enhance cytotoxicity in TFE3-RCC cells, a low dose of a cancer drug should be sufficient to minimize the damage for non-cancer cells, while effectively eliminating the *PRCC-TFE3* expressing cancer cells.

In summary, our data revealed a novel pathway in which PRCC-TFE3 transcription is responsible for chemoresistance in Xp11.2 translocation RCC. In addition, we have developed a potential chemical inhibitor of PRCC-TFE3 transcription, Chb16, using a novel PI-based approach, which can sensitize cancer cells to apoptosis when in combination with a cancer drug such as etoposide. Further improvement of the selectivity of this type of chemical inhibitor is still necessary. Overall, we propose that our identification of novel PIP-Chb-based inhibitors could provide the foundation for effective forms of therapy for advanced TFE3-fusion RCC and other types of translocation RCC tumors through targeting chemoresistance.

DISCLOSURE

Sally Mehanna received a scholarship from Tokyo Biochemical Research Foundation (TBRF).

ORCID

Yasuhiko Kamikubo https://orcid.org/0000-0003-2761-8508
Hisashi Hasumi https://orcid.org/0000-0001-8211-8835
Masaya Baba https://orcid.org/0000-0002-5308-6683

REFERENCES

1. Renal IK. Renal cell tumors: Understanding their molecular pathological epidemiology and the 2016 WHO classification. *Int J Mol Sci.* 2016;18(10):2195.
2. Sidhar SK, Clark J, Gill S, et al. The t(X;1)(p11.2;q21.2) translocation in papillary renal cell carcinoma fuses a novel gene PRCC to the TFE3 transcription factor gene. *Hum Mol Genet.* 1996;5:1333-1338.
3. Lopez-Beltran A, Scarpelli M, Montironi R, Kirkali Z. 2004 WHO classification of the renal tumors of the adults. *Eur Urol.* 2006;49:798-805.
4. Cajaiba MM, Dyer LM, Geller JI, et al. The classification of pediatric and young adult renal cell carcinomas registered on the children's oncology group (COG) protocol AREN03B2 after focused genetic testing. *Cancer.* 2018;124:3381-3389.
5. Komai Y, Fujiwara M, Fujii Y, et al. Adult Xp11 translocation renal cell carcinoma diagnosed by cytogenetics and immunohistochemistry. *Clin Cancer Res.* 2009;15:1170-1176.
6. Kauffman EC, Ricketts CJ, Rais-Bahrami S, et al. Molecular genetics and cellular features of TFE3 and TFEB fusion kidney cancers. *Nat Rev Urol.* 2014;11:465-475.
7. Ross H, Argani P. Xp11 translocation renal cell carcinoma. *Pathology.* 2010;42:369-373.
8. Clark J, Lu YJ, Sidhar SK, et al. Fusion of splicing factor genes PSF and NonO (p54nrb) to the TFE3 gene in papillary renal cell carcinoma. *Oncogene.* 1997;15:2233-2239.
9. Sun G, Chen J, Liang J, et al. Integrated exome and RNA sequencing of TFE3-translocation renal cell carcinoma. *Nat Commun.* 2021;12:5262.
10. Tanaka M, Homme M, Yamazaki Y, Shimizu R, Takazawa Y, Nakamura T. Modeling alveolar soft part sarcoma unveils novel mechanisms of metastasis. *Can Res.* 2017;77:897-907.
11. Martina JA, Diab HI, Lishu L, et al. The nutrient-responsive transcription factor TFE3 promotes autophagy, lysosomal biogenesis, and clearance of cellular debris. *Sci Signal.* 2014;7:ra9.
12. Settembre C, Fraldi A, Medina DL, Ballabio A. Signals from the lysosome: a control centre for cellular clearance and energy metabolism. *Nat Rev Mol Cell Biol.* 2013;14:283-296.
13. Pastore N, Vainshtein A, Klisch TJ, et al. TFE3 regulates whole-body energy metabolism in cooperation with TFEB. *EMBO Mol Med.* 2017;9:605-621.
14. Settembre C, De Cegli R, Mansueto G, et al. TFEB controls cellular lipid metabolism through a starvation-induced autoregulatory loop. *Nat Cell Biol.* 2013;15:647-658.
15. Pisonero-Vaquero S, Soldati C, Cesana M, Ballabio A, Medina DL. TFEB modulates p21/WAF1/CIP1 during the DNA damage response. *Cells.* 2020;9:1186.
16. Yin Q, Jian Y, Xu M, et al. CDK4/6 regulate lysosome biogenesis through TFEB/TFE3. *J Cell Biol.* 2020;219:e201911036.
17. Brady OA, Jeong E, Martina JA, Pirooznia M, Tunc I, Puertollano R. The transcription factors TFE3 and TFEB amplify p53 dependent transcriptional programs in response to DNA damage. *eLife.* 2018;7:40856.
18. Baba M, Furuya M, Motoshima T, et al. TFE3 Xp11.2 translocation renal cell carcinoma mouse model reveals novel therapeutic targets and identifies GPNMB as a diagnostic marker for human disease. *Mol Cancer Res.* 2019;17:1613-1626.
19. Kurahashi R, Kadomatsu T, Baba M, et al. MicroRNA-204-5p: A novel candidate urinary biomarker of Xp11.2 translocation renal cell carcinoma. *Cancer Sci.* 2019;110:1897-1908.
20. Fellmann C, Hoffmann T, Sridhar V, et al. An optimized microRNA backbone for effective single-copy RNAi. *Cell Rep.* 2013;5:1704-1713.
21. Morita K, Suzuki K, Maeda S, et al. Genetic regulation of the RUNX transcription factor family has antitumor effects. *J Clin Investig.* 2017;127:2815-2828.
22. Liberzon A, Birger C, Thorvaldsdóttir H, Ghandi M, Mesirov JP, Tamayo P. The Molecular Signatures Database (MSigDB) hallmark gene set collection. *Cell Syst.* 2015;1:417-425.
23. Baba M, Hong SB, Sharma N, et al. Folliculin encoded by the BHD gene interacts with a binding protein, FNIP1, and AMPK, and is

involved in AMPK and mTOR signaling. *Proc Natl Acad Sci USA*. 2006;103:15552-15557.

24. Ishiguro N, Yoshida H. ASPL-TFE3 oncoprotein regulates cell cycle progression and induces cellular senescence by up-regulating p21. *Neoplasia*. 2016;18:626-635.

25. Campbell NK, Fitzgerald HK, Dunne A. Regulation of inflammation by the antioxidant haem oxygenase 1. *Nat Rev Immunol*. 2021;21:411-425.

26. Zhu XF, Li W, Ma JY, et al. Knockdown of heme oxygenase-1 promotes apoptosis and autophagy and enhances the cytotoxicity of doxorubicin in breast cancer cells. *Oncol Lett*. 2015;10:2974-2980.

27. Bukowska-Strakova K, Włodek J, Pitera E, et al. Role of HMOX1 promoter genetic variants in chemoresistance and chemotherapy induced neutropenia in children with acute lymphoblastic leukemia. *Int J Mol Sci*. 2021;22(3):988.

28. Trauger JW, Baird EE, Dervan PB. Recognition of DNA by designed ligands at subnanomolar concentrations. *Nature*. 1996;382:559-561.

29. Hidaka T, Sugiyama H. Chemical approaches to the development of artificial transcription factors based on pyrrole-imidazole polyamides. *Chem Rec*. 2021;21:1374-1384.

30. Nakagawa Y, Shimano H, Yoshikawa T, et al. TFE3 transcriptionally activates hepatic IRS-2, participates in insulin signaling and ameliorates diabetes. *Nat Med*. 2006;12:107-113.

31. Damayanti NP, Budka JA, Khella HWZ, et al. Therapeutic targeting of TFE3/IRS-1/PI3K/mTOR axis in translocation renal cell carcinoma. *Clin Can Res*. 2018;24:5977-5989.

32. Chen J. The cell-cycle arrest and apoptotic functions of p53 in tumor initiation and progression. *Cold Spring Harb Perspect Med*. 2016;6: a026104.

33. Bieging KT, Attardi LD. Deconstructing p53 transcriptional networks in tumor suppression. *Trends Cell Biol*. 2012;22:97-106.

34. Freund A, Laberge RM, Demaria M, Campisi J. Lamin B1 loss is a senescence-associated biomarker. *Mol Biol Cell*. 2012;23:2066-2075.

35. Coppé JP, Desprez PY, Krtolica A, Campisi J. The senescence-associated secretory phenotype: the dark side of tumor suppression. *Annu Rev Pathol*. 2010;5:99-118.

36. Kumari R, Jat P. Mechanisms of cellular senescence: cell cycle arrest and senescence associated secretory phenotype. *Front Cell Develop Biol*. 2021;9: 645593.

37. Karpinich NO, Tafani M, Rothman RJ, Russo MA, Farber JL. The course of etoposide-induced apoptosis from damage to DNA and p53 activation to mitochondrial release of cytochrome c. *J Biol Chem*. 2002;277:16547-16552.

38. Brasseur K, Gévry N, Asselin E. Chemoresistance and targeted therapies in ovarian and endometrial cancers. *Oncotarget*. 2017;8:4008-4042.

39. Lu C, Shervington A. Chemoresistance in gliomas. *Mol Cell Biochem*. 2008;312:71-80.

40. Tenhunen R, Marver HS, Schmid R. The enzymatic conversion of heme to bilirubin by microsomal heme oxygenase. *Proc Natl Acad Sci USA*. 1968;61:748-755.

41. Doi K, Akaike T, Fujii S, et al. Induction of haem oxygenase-1 nitric oxide and ischaemia in experimental solid tumours and implications for tumour growth. *Br J Cancer*. 1999;80:1945-1954.

42. Maines MD, Abrahamsson PA. Expression of heme oxygenase-1 (HSP32) in human prostate: normal, hyperplastic, and tumor tissue distribution. *Urology*. 1996;47:727-733.

43. Torisu-Itakura H, Furue M, Kuwano M, Ono M. Co-expression of thymidine phosphorylase and heme oxygenase-1 in macrophages in human malignant vertical growth melanomas. *Jpn J Cancer Res*. 2000;91:906-910.

44. Hara E, Takahashi K, Tominaga T, et al. Expression of heme oxygenase and inducible nitric oxide synthase mRNA in human brain tumors. *Biochem Biophys Res Commun*. 1996;224:153-158.

45. Taguchi K, Yamamoto M. The KEAP1-NRF2 system in cancer. *Front Oncol*. 2017;7:85.

46. Reichard JF, Motz GT, Puga A. Heme oxygenase-1 induction by NRF2 requires inactivation of the transcriptional repressor BACH1. *Nucleic Acids Res*. 2007;35:7074-7086.

47. Linehan WM, Spellman PT, Ricketts CJ, et al. Comprehensive molecular characterization of papillary renal-cell carcinoma. *N Engl J Med*. 2016;374:135-145.

48. Liu F, Fu Y, Meyskens FLJr. MiTF regulates cellular response to reactive oxygen species through transcriptional regulation of APE-1/Ref-1. *J Invest Dermatol*. 2009;129:422-431.

49. Wang H, Wang N, Xu D, et al. Oxidation of multiple MiT/TFE transcription factors links oxidative stress to transcriptional control of autophagy and lysosome biogenesis. *Autophagy*. 2020;16:1683-1696.

50. Zhang X, Cheng X, Yu L, et al. MCOLN1 is a ROS sensor in lysosomes that regulates autophagy. *Nat Commun*. 2016;7:12109.

51. Wang B, Yin X, Gan W, et al. PRCC-TFE3 fusion-mediated PRKN/parkin-dependent mitophagy promotes cell survival and proliferation in PRCC-TFE3 translocation renal cell carcinoma. *Autophagy*. 2021;17:2475-2493.

52. Ellis CL, Eble JN, Subhawong AP, et al. Clinical heterogeneity of Xp11 translocation renal cell carcinoma: impact of fusion subtype, age, and stage. *Modern Pathol*. 2014;27:875-886.

53. Ambalavanan M, Geller JI. Treatment of advanced pediatric renal cell carcinoma. *Pediatr Blood Cancer*. 2019;66:e27766.

54. Procopiou G, Procopiou PA. *Chapter 1 Synthetic Approaches and Challenges to Transcription Factor Inhibitors. Small-molecule Transcription Factor Inhibitors in Oncology*. The Royal Society of Chemistry; 2019:1-41.

SUPPORTING INFORMATION

Additional supporting information may be found in the online version of the article at the publisher's website.